Electronic Supplementary Material (ESI) for Journal of Materials Chemistry A.

# Fusion or non-fusion of quasi-two-dimensional fused perylene diimide acceptors: the importance of molecular geometry for fullerene-free organic solar cells

Yuli Yin,‡[a] Zhi Zheng,‡[a] Daoyuan Chen,[a] Ming Liu,[a] Jianqi Zhang,[b] Fengyun Guo,[a] Shiyong Gao,[a] Liancheng Zhao,[a] Yong Zhang[a,c*]

[a] *School of Materials Science and Engineering, Harbin Institute of Technology, Harbin 150001, China*

[b] *Key Laboratory of Nanosystem and Hierarchical Fabrication, National Center for Nanoscience and Technology, Beijing 100190, China*

[c] *School of Materials Science and Engineering, Zhengzhou University, Zhengzhou 450001, China*

*Corresponding authors (email: yongzhang@hit.edu.cn)

‡ Both authors contributed equally to this work.

## EXPERIMENTAL SECTION

### Characterization

$^1$H NMR spectra were recorded on a Bruker AV600 NMR spectrometer and used tetramethylsilane (TMS) as an internal standard in $CDCl_3$. The UV-Vis spectra of polymers were measured on with a TU-1601 spectrophotometer by using a 1 cm glass cuvette. The solution UV-Vis absorption spectra at elevated temperature were collected with a Perkin Elmer Lambda 950 UV/VIS/NIR Spectrophotometer (USA). Cyclic voltammetry (CV) was performed in 0.1M tetrabutylammonium hexafluorophosphate in acetonitrile at a scan rate of 100 mV/s with ITO as the working electrode, Pt wire as the counter electrode and $Ag/Ag^+$ as the reference electrode. Atomic force microscopy (AFM) images were obtained using a NanoMan VS microscope in the tapping mode. Transmission electron microscopy (TEM) measurements were performed on a Hitachi H-7650 instrument (Hitachi Company, Japan). GIWAXS measurements were conducted at XEUSS SAXS/WAXS system with X-ray wavelength of 1.5418 Å. The film samples were irradiated at a fixed angle of 0.2° for 12 hours.

***Device Fabrication.*** Prepatterned ITO-coated glasses were cleaned by sequential cycles of sonication in soap water, deionized water, ethanol, acetone, and isopropanol for 30 min, respectively. After UV/ozone treatment for 6 min, PEDOT:PSS hole transport layer was filtered and spin-coated on top of the treated-ITO at 4000 rpm for 25 s and dried over 160 $^{o}$C for 20 min. The active layer solutions were prepared in CB (with a polymer concentration of 8 mg/mL and a D/A ratio at 1:1.5), and spin-coated on the PEDOT:PSS-coated substrates in a glove-box under $N_2$ atmosphere at 1500 rpm for 45 s to obtain a thickness of $\approx$120 nm. The blend films were then transferred to the heating platform and annealed at 100 $^{o}$C for 10 min. A thin layer of PFN-Br (1 mg/mL) was spin coated on the top of active layer with 4000 rpm for 30 s. Finally, the Ag (100 nm) electrode was evaporated onto the active layer under a vacuum of $10^{-5}$ Torr. The current-voltage characteristics of the devices were measured using a computer-controlled Keithley 2400 source meter under stimulated AM1.5 G at an intensity of 100 mW/cm$^2$ provided by a solar simulator. The EQEs were measured by an Oriel Newport System. All above measurements were done at room temperature.

The hole-only device for the hole mobility was fabricated with a device structure of ITO/PEDOT:PSS/PTB7-Th:SMAs/Au. The electron-only device for the electron mobility was fabricated with a device structure of ITO/ZnO/PTB7-Th: SMAs /PFN-Br/AI. Both the hole and electron mobilities by space charge limited current (SCLC) were calculated with the following Mott-Gurney equation in the SCLC region: $J = (9/8)\varepsilon_0\varepsilon_r\mu(V^2/L^3)$, in which $\varepsilon_0$ is the permittivity of the vacuum, $\varepsilon_r$ is the dielectric constant of the polymer and assumed to be 3, and $L$ is the thickness of active layer.

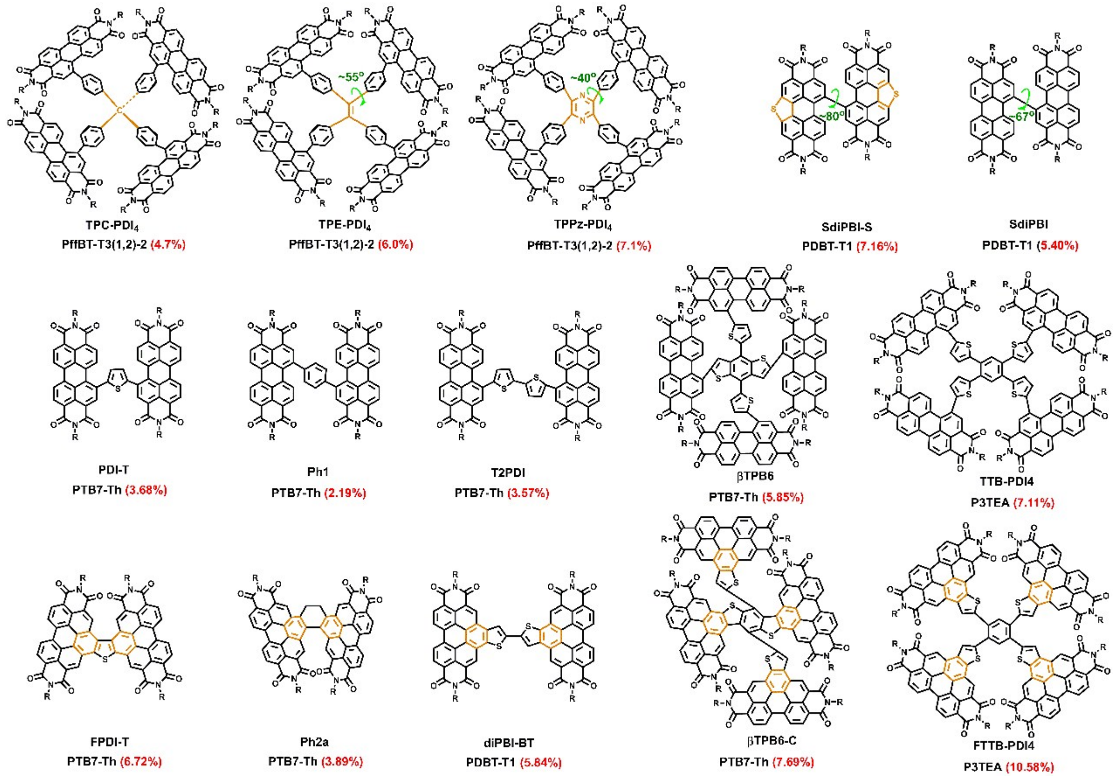

**Fig. S1.** The previous work on PDI-based fullerene-free electron acceptors via control of the molecular geometries.

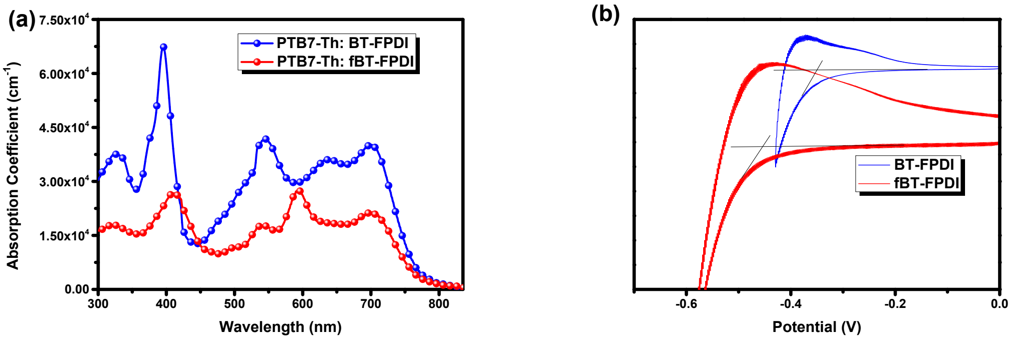

**Fig. S2.** a) The absorption coefficient of BT-FPDI and fBT-FPDI blend films. b) The cyclic voltammetry of BT-FPDI and fBT-FPDI in thin film.

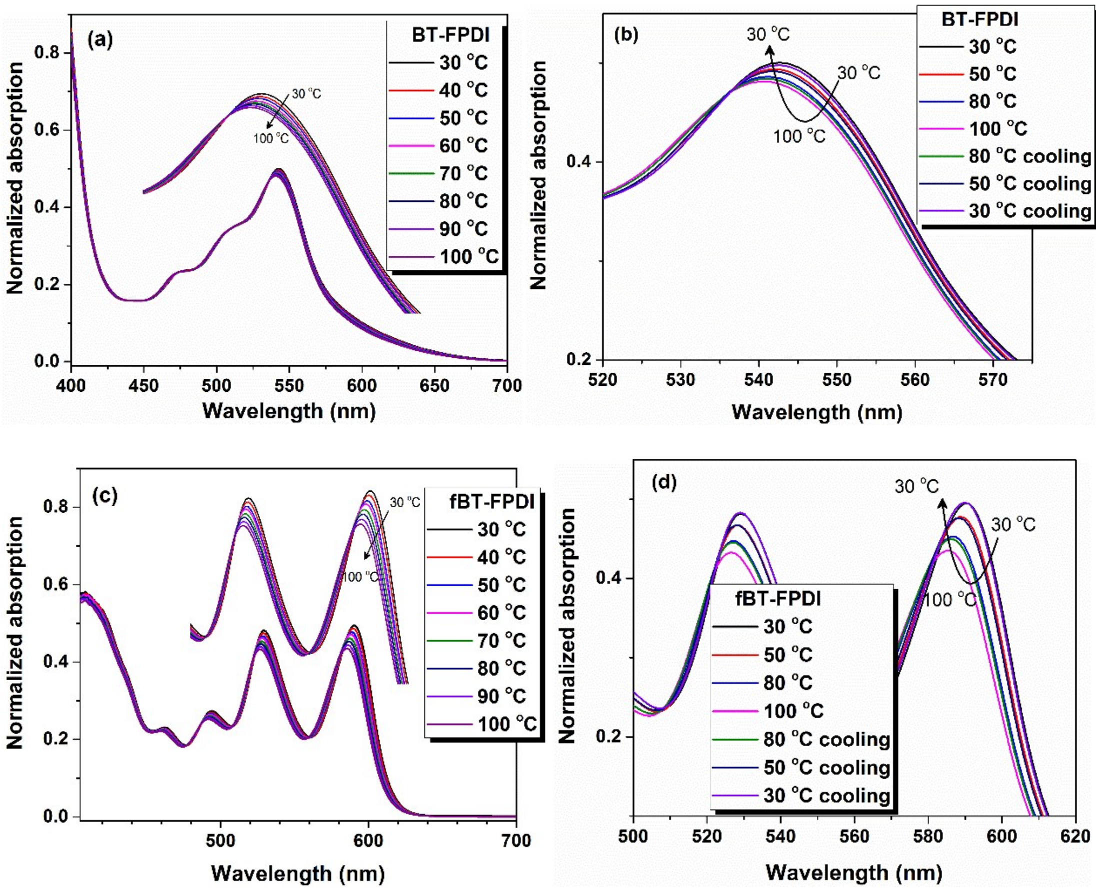

**Fig. S3.** The temperature-dependent UV-vis absorption of BT-FPDI and fBT-FPDI in chlorobenzene solution. (a) BT-FPDI from 30 °C to 100 °C; (b) BT-FPDI cooling from 100 °C to 30 °C; (c) fBT-FPDI from 30 °C to 100 °C; (d) fBT-FPDI cooling from 100 °C to 30 °C.

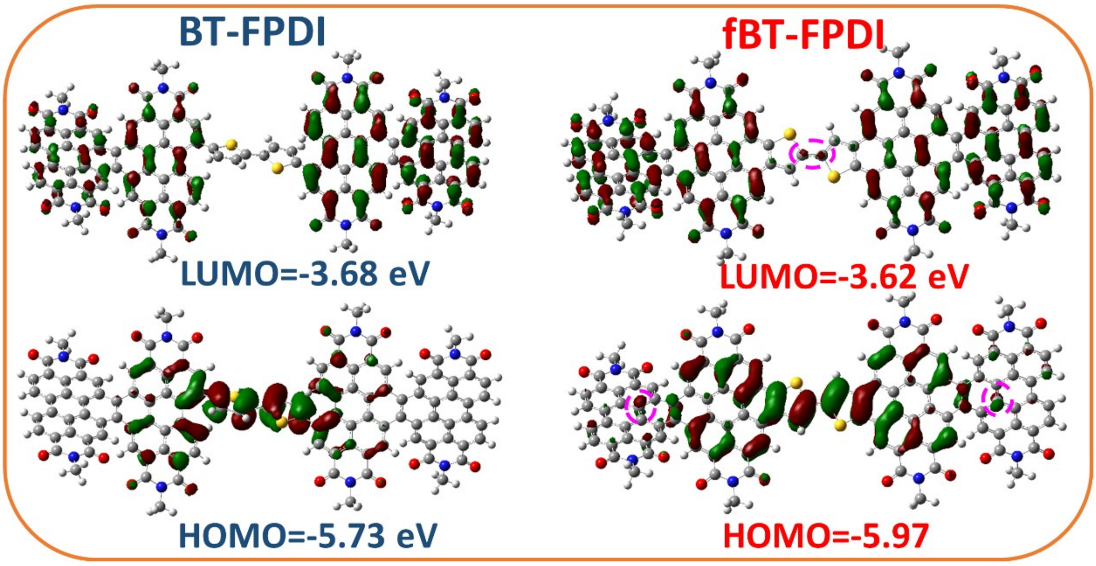

**Fig. S4.** LUMO and HOMO ene4rgy levels of BT-FPDI and fBT-FPDI calculated by DFT/B3LYP/6-31G.

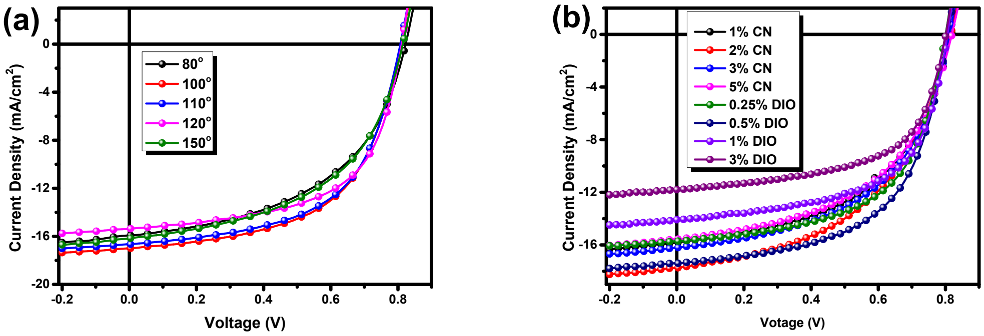

**Fig. S5.** The current density-voltage curves of PTB7-Th:BT-FPDI device by treated with different annealing temperatures (a) and various volume fraction of additives (b).

**Table S1** The photovoltaic performances of fullerene-free OSCs based on PTB7-Th:BT-FPDI with different annealing temperatures and the additive.

| **Temperature** | **Additive** | **$V_{oc}$ (V)** | **$J_{sc}$(mA/cm$^2$)** | **FF (%)** | **PCE (%)** |
|---|---|---|---|---|---|
| 80$^{o}$ | w/o | 0.82 | 15.91 | 50.40 | 6.59 |
| **100$^{o}$** | **w/o** | **0.81** | **16.96** | **56.90** | **7.80** |
| 110$^{o}$ | w/o | 0.81 | 16.62 | 57.4 | 7.69 |
| 120$^{o}$ | w/o | 0.81 | 15.3 | 59.29 | 7.38 |
| 150$^{o}$ | w/o | 0.81 | 16.12 | 51.37 | 6.74 |
| 100$^{o}$ | 1%CN | 0.81 | 15.76 | 51.44 | 6.60 |
| 100$^{o}$ | 2%CN | 0.81 | 17.65 | 50.10 | 7.19 |
| 100$^{o}$ | 3%CN | 0.81 | 16.16 | 52.40 | 6.87 |
| 100$^{o}$ | 5%CN | 0.82 | 15.51 | 51.34 | 6.51 |
| 100$^{o}$ | 0.25%DIO | 0.80 | 15.68 | 58.2 | 7.30 |
| **100$^{o}$** | **0.5%DIO** | **0.81** | **17.35** | **57.67** | **8.07** |
| 100$^{o}$ | 1%DIO | 0.81 | 14.07 | 59.9 | 6.75 |
| 100$^{o}$ | 3%DIO | 0.80 | 11.80 | 59.4 | 5.61 |

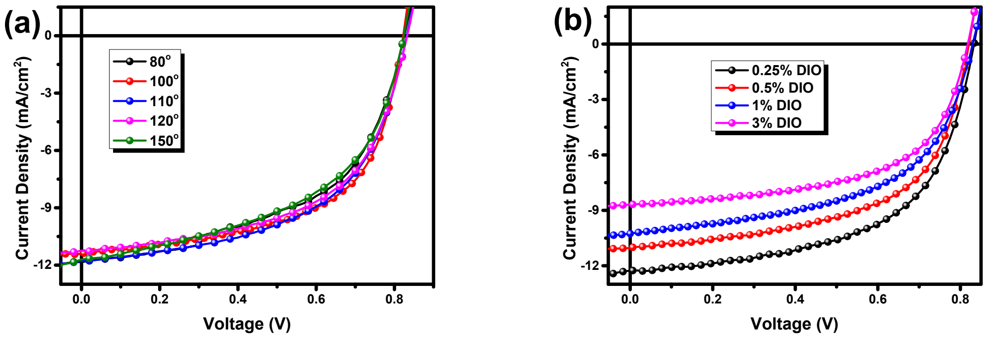

**Fig. S6.** The current density-voltage curves of PTB7-Th:fBT-FPDI device by treated with different annealing temperatures (a) and various volume fraction of additive (b).

.

**Table S2** The photovoltaic performances of fullerene-free OSCs based on PTB7-Th:fBT-FPDI with different annealing temperatures and the additive.

| Temperature | Additive | $V_{oc}$ (V) | $J_{sc}$(mA/cm$^2$) | FF (%) | PCE (%) |
|---|---|---|---|---|---|
| 80° | w/o | 0.82 | 11.84 | 52.09 | 5.06 |
| **100°** | **w/o** | **0.82** | **11.36** | **58.64** | **5.47** |
| 110° | w/o | 0.82 | 11.79 | 55.66 | 5.38 |
| 120° | w/o | 0.82 | 11.27 | 56.64 | 5.23 |
| 150° | w/o | 0.82 | 11.7 | 51.22 | 4.92 |
| **100°** | **0.25%DIO** | **0.83** | **12.30** | **57.50** | **5.89** |
| 100° | 0.5%DIO | 0.82 | 11.00 | 57.90 | 5.23 |
| 100° | 1%DIO | 0.82 | 10.26 | 55.2 | 4.64 |
| 100° | 3%DIO | 0.82 | 8.68 | 58.44 | 4.15 |

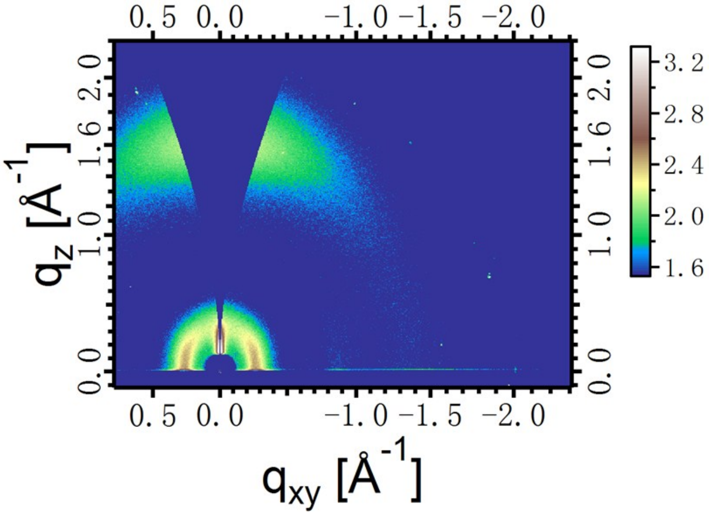

**Fig. S7.** Two-dimensional (2D) GIWAXS pattern of PTB7-Th (a), and azimuth intensity profiles of BT-FPDI and fBT-FPDI for both pristine and blend film (b).

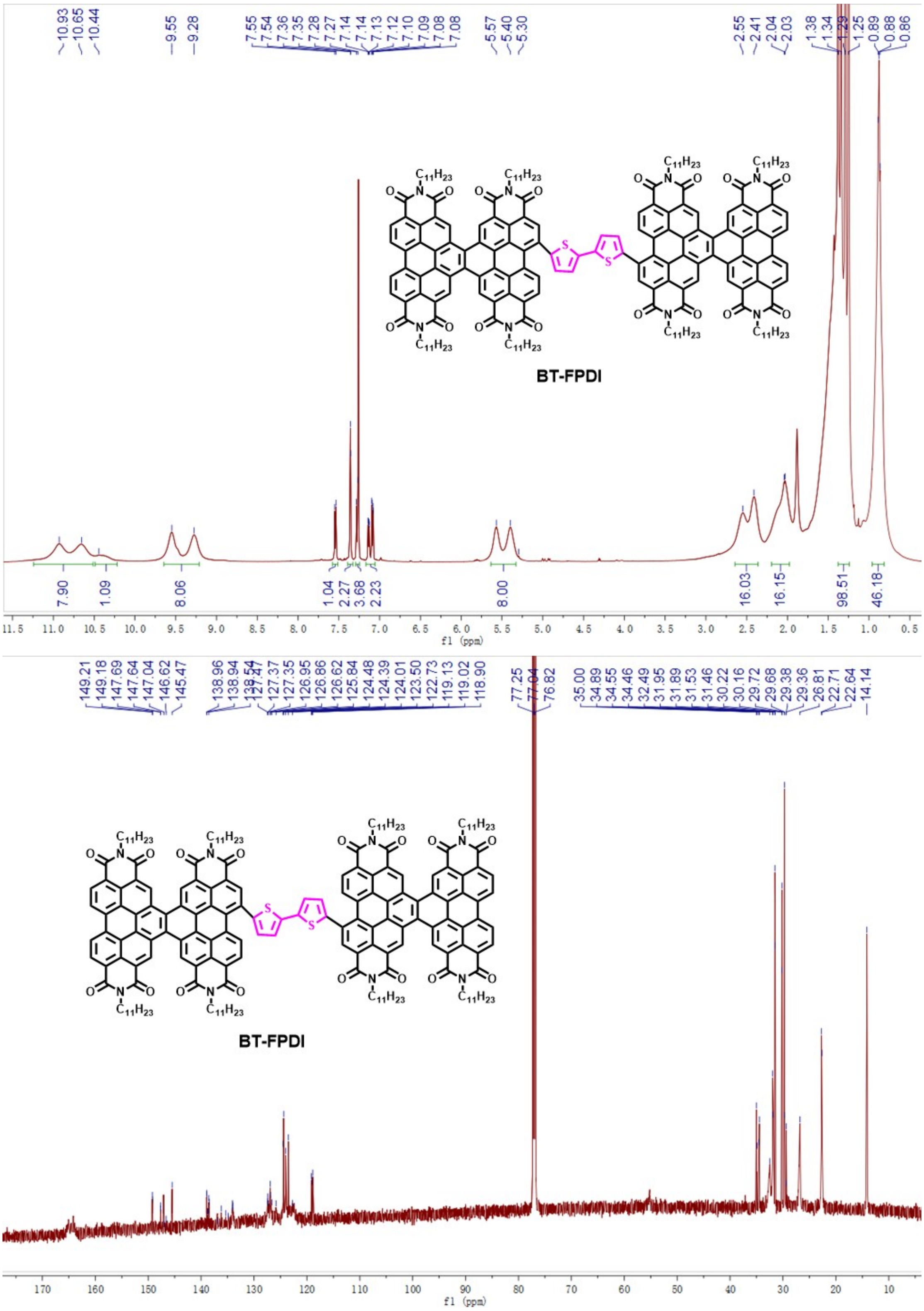

**Fig. S8.** The $^1$H NMR and $^{13}$C NMR spectra of BT-FPDI.

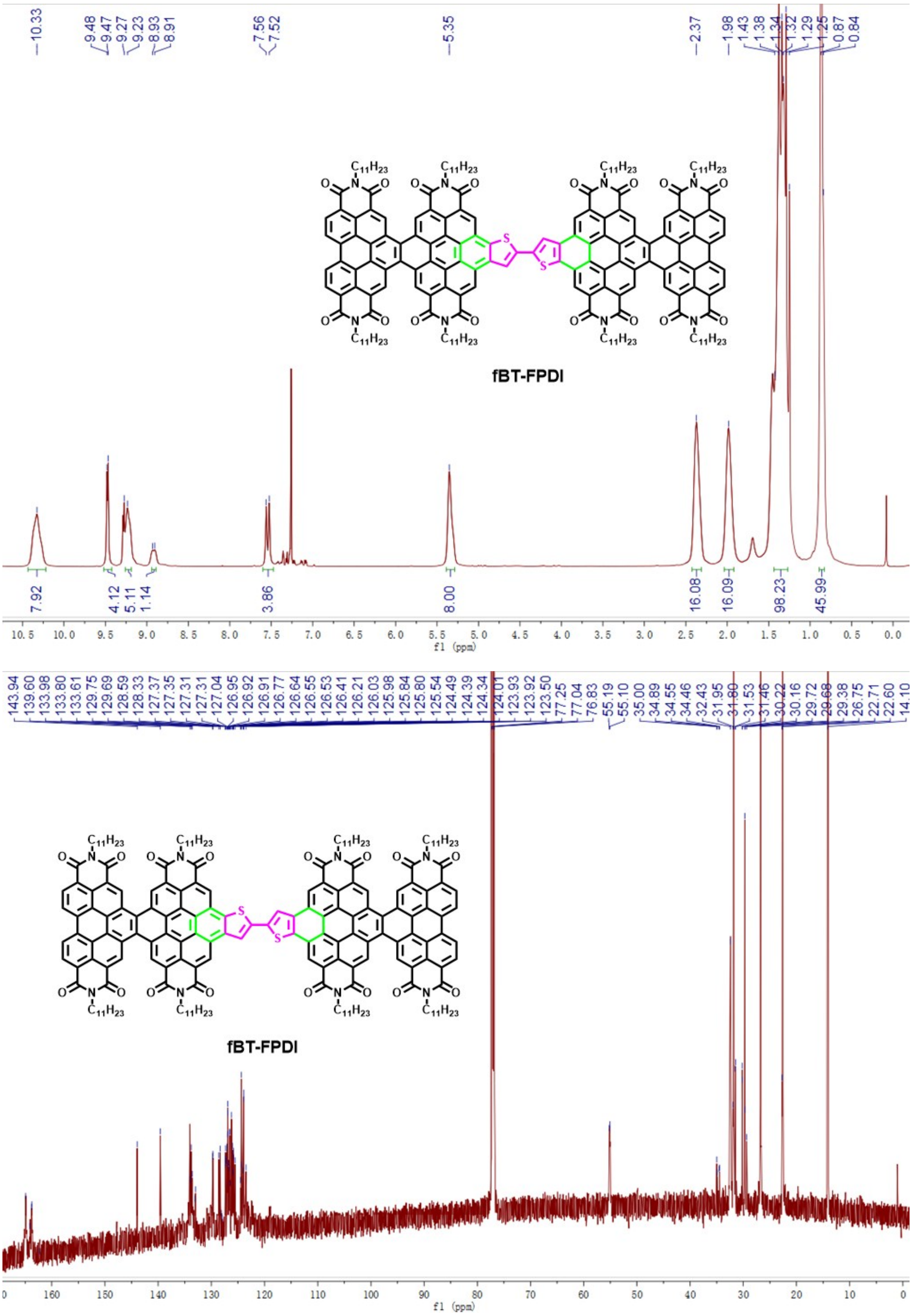

**Fig. S9.** The $^{1}$H NMR and $^{13}$C NMR spectra of fBT-FPDI.